FINE STRUCTURE WITHIN THE REDSHIFT-MAGNITUDE CORRELATION FOR GALAXIES

W. G. TIFFT

Steward Observatory, University of Arizona, Tucson, Ariz. 85721, U.S.A.

Abstract. Previous work on the redshift-magnitude banding correlation is briefly reviewed. New tests of the concept are applied successfully to a second cluster (A2199) and the outer portions of the Coma cluster. Using more than 200 redshifts in Coma, Perseus, and A2199 the presence of a distinct band-related-periodicity in redshift is indicated. Finally, a new sample of accurate redshifts of bright Coma galaxies on a single band is presented, which shows a strong redshift periodicity of 220 km s^{-1}. An upper limit of 20 km s^{-1} is placed on the internal Doppler component of motion in the Coma cluster.

Redshift-magnitude bands are, therefore, now recognized to consist of discrete 'spin states' organized into 'spin groups' which show strong morphological associations. Bands are probably in turn organized into band systems. The individual spin states are suggested to represent distinct configurations of matter at the nuclear or fundamental particle structure level. Transitions between states in a time systematic sense of decreasing redshift (increasing internal binding) are suggested to occur in galaxy nuclei. Energy released in such transitions may be the driving energy in radio sources and related objects.

Investigations of the Coma cluster have played and continue to play a major role in the development of intrinsic redshift concepts which I shall present here. Figure 1 is a reminder of the original Coma cluster observations (Tifft, 1972) which introduced two of the basic phenomena, the nuclear-magnitude-redshift bands and the morphological separation of galaxies along the band direction, both correlations being statistically quite significant.

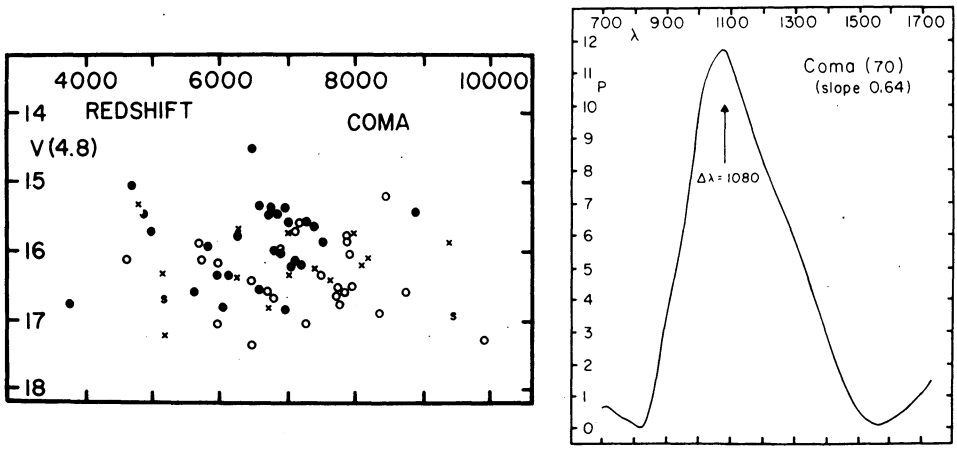

Fig. 1. (left) The original Coma cluster core redshift-magnitude diagram (Tifft, 1972) showing banding and morphological separation along the bands. Symbols denote morphology: filled circles = E, open circles = S0, X = SB0, and S = spiral. (right) Power spectrum of the redshift distribution of the core sample of 70 galaxies projected to a uniform magnitude along a slope of 0.64 mag per 1000 km s^{-1}. The projection slope corresponds to the direction of maximum morphological separation. The probability of finding such a peak by accident in a power spectrum is about 0.0005.

John R. Shakeshaft (ed.), The Formation and Dynamics of Galaxies. 243–256.

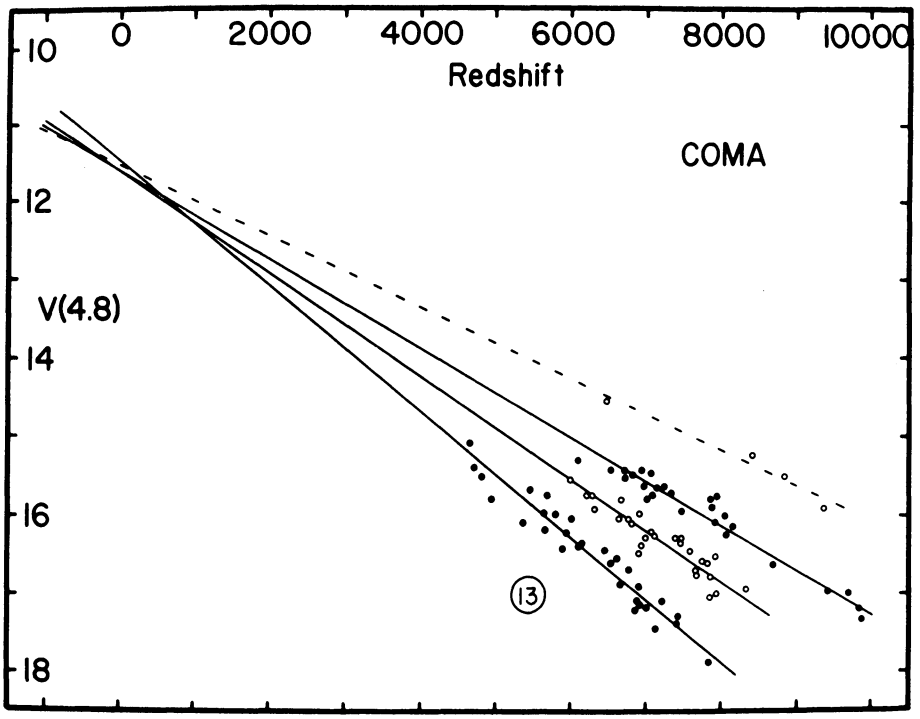

Fig. 2. The extended Coma cluster core redshift-magnitude diagram (Tifft, 1973a) showing convergence of the bands toward zero redshift. Alternate bands are shown with alternate symbols and 13 points below the main bands are omitted. The convergence toward zero suggests that the bands are scaled intrinsic phenomena with no significant Doppler component.

With the extension of the Coma cluster sample (Tifft, 1973a) came one of the first direct evidences that the entire redshift phenomena could be an intrinsic property of matter and completely or nearly completely non-Doppler. Figure 2 illustrates the convergence of the bands toward zero redshift, permitting their interpretation as scaled versions of one another with no major Doppler component. This was further strengthened by the investigation of QSS objects (Tifft, 1973b). Figure 3 illustrates the concept of bands organized into convergent band systems which can be visible in an all-sky sample only if the redshift is virtually entirely non-Doppler, and matter and galaxies evolve systematically in cosmic time.

On the basis of the band properties, slope and spacing observed in Coma, and the universal band concept, specific predictions concerning bands in other clusters can be made. Figure 4 shows such a test for the A2199 cluster (Tifft, 1974). Power spectral analysis at the predicted slope and spacing confirms the bands with a probability of 10^{-3}. The cluster also shows morphological separation as in Coma.

One of the areas which has caused some discussion relates to the difficulty in seeing band effects in total magnitudes. For example, Figure 5 shows a sample of all brighter galaxies with known redshifts within 6° of the Coma cluster centre (Tifft,

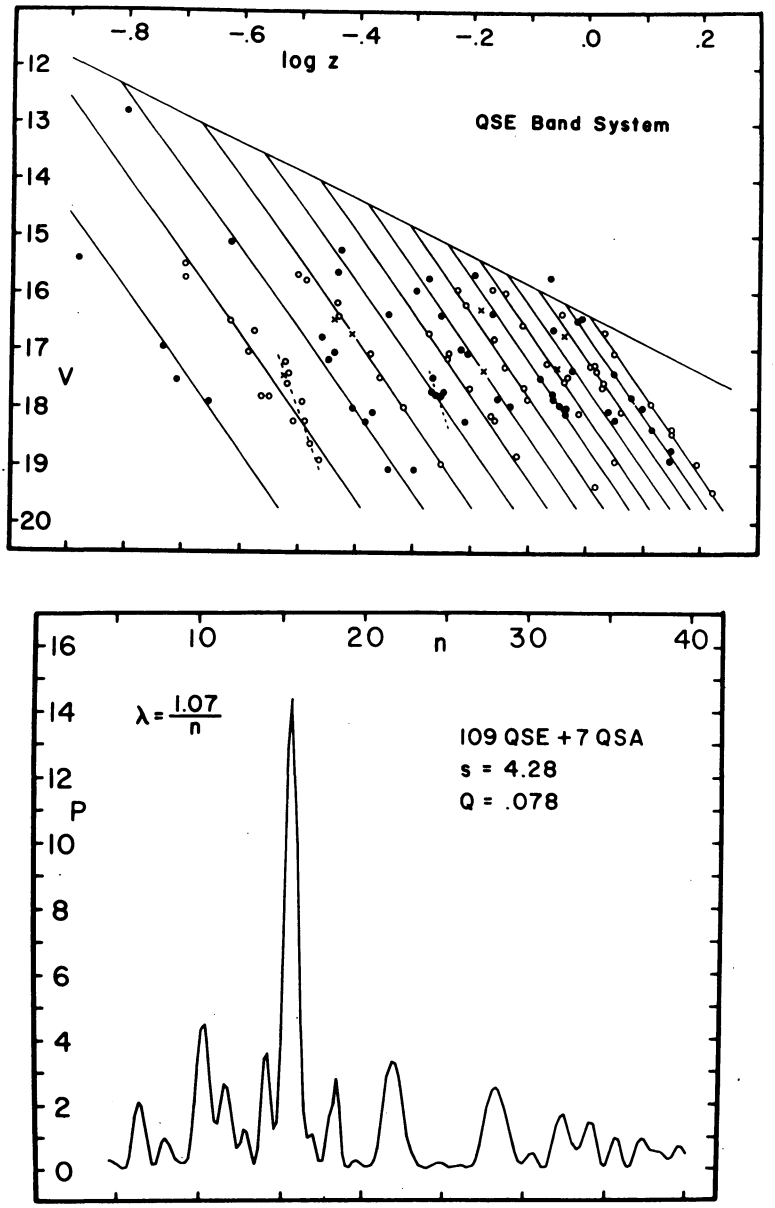

Fig. 3. (upper) Suggested organization of QSS redshifts and magnitudes into a system of bands (Tifft, 1973b) as an entirely intrinsic phenomenon. (lower) Power spectrum of the QSS distribution illustrated after projection to a uniform magnitude along a slope $s=4.28$ mag per factor of two in redshift and 'linearized' by a quadratic stretching factor Q (i.e. $z''=z'+Q(z')^2$ where z' is the value of z projected to $V=16.2$). Although the details of the higher bands are probably doubtful, the lower z bands appear distinct. (QSE refers to quasi-stellar emission-line objects and QSA to quasi-stellar absorption-line objects).

https://doi.org/10.1017/S0074180900024499 Published online by Cambridge University Press

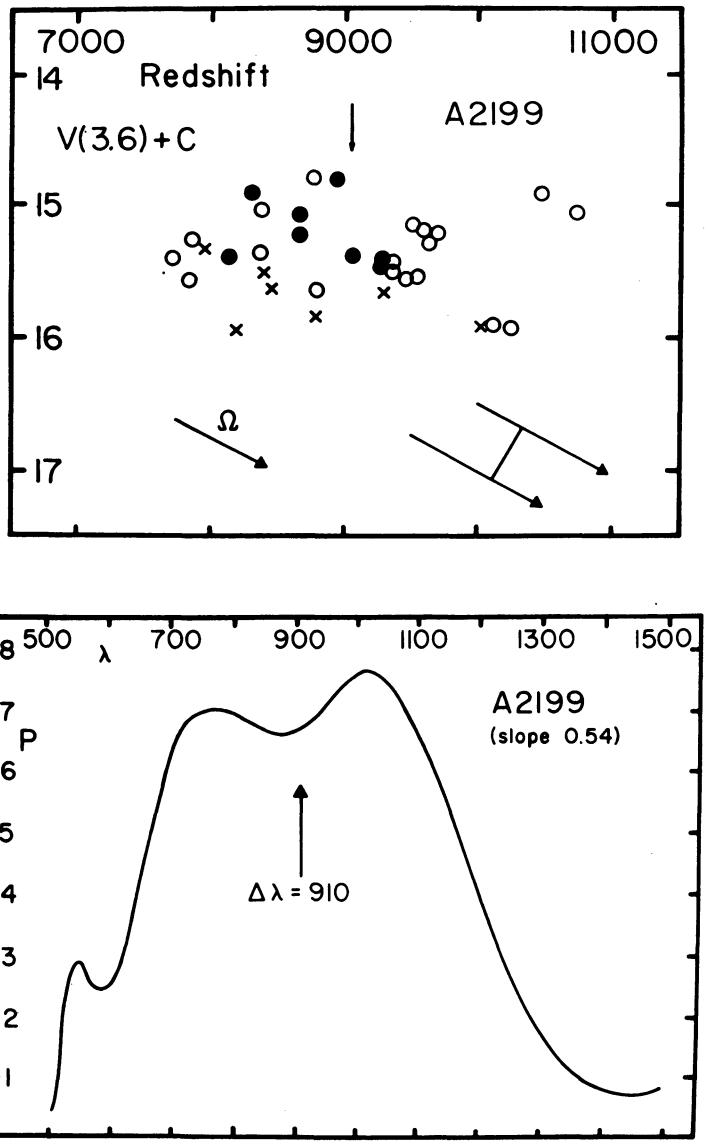

Fig. 4. (upper) Redshift-nuclear magnitude diagram for galaxies in the core of the A2199 cluster (Tifft, 1974). Magnitudes refer to the central 3.″6 region of each galaxy and are uncertain within a constant. The band direction and spacing predicted from Coma are shown with the coupled vectors. The single vector labelled Ω denotes the direction of morphological separation in the sample (filled circles = E galaxies, open circles = non-E galaxies, X = unclassified) which is identical to the band direction as seen in Coma. The downward pointing vector marks the mean cluster redshift. (lower) Power spectrum of the redshift distribution in the A2199 sample projected at the predicted slope and wavelength. The probability of finding a power of 7 at the predicted wavelength in a random sample is 10^{-3}.

https://doi.org/10.1017/S0074180900024499 Published online by Cambridge University Press

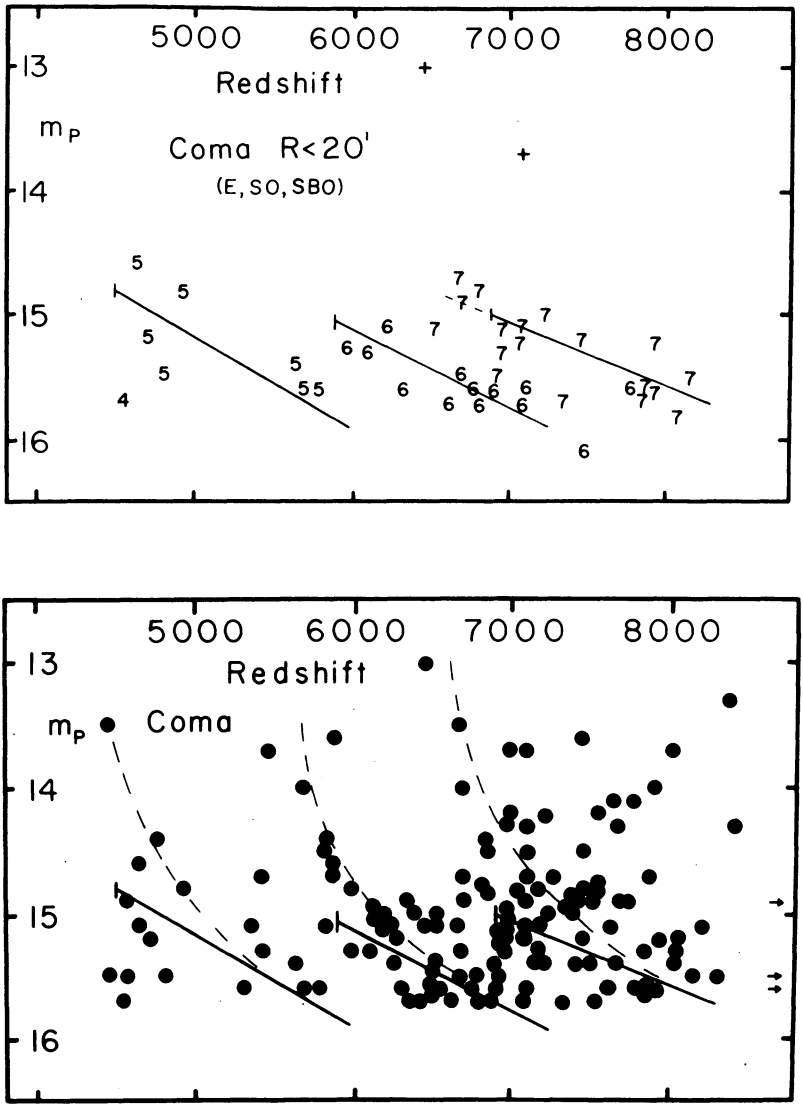

Fig. 5. (lower) Redshift-magnitude (m_p) diagram for all Coma galaxies within 6° of the cluster centre which have known redshifts and published m_p magnitudes (see Tifft, 1974). (upper) Redshift-magnitude (m_p) diagram for all E, S0, or SB0 galaxies in the above mentioned sample which are in common with central region studies and hence have a band assignment, indicated by the numerical symbol. The two supergiant galaxies are shown with crosses. The overlap objects along with known band spacing and convergence permit the mapping of mean band location lines into the diagram. These mean lines and suggested curving extensions are repeated on the lower figure. No obvious banding appears in the lower figure, although association of galaxies with the curved extensions is suggested.

https://doi.org/10.1017/S0074180900024499 Published online by Cambridge University Press

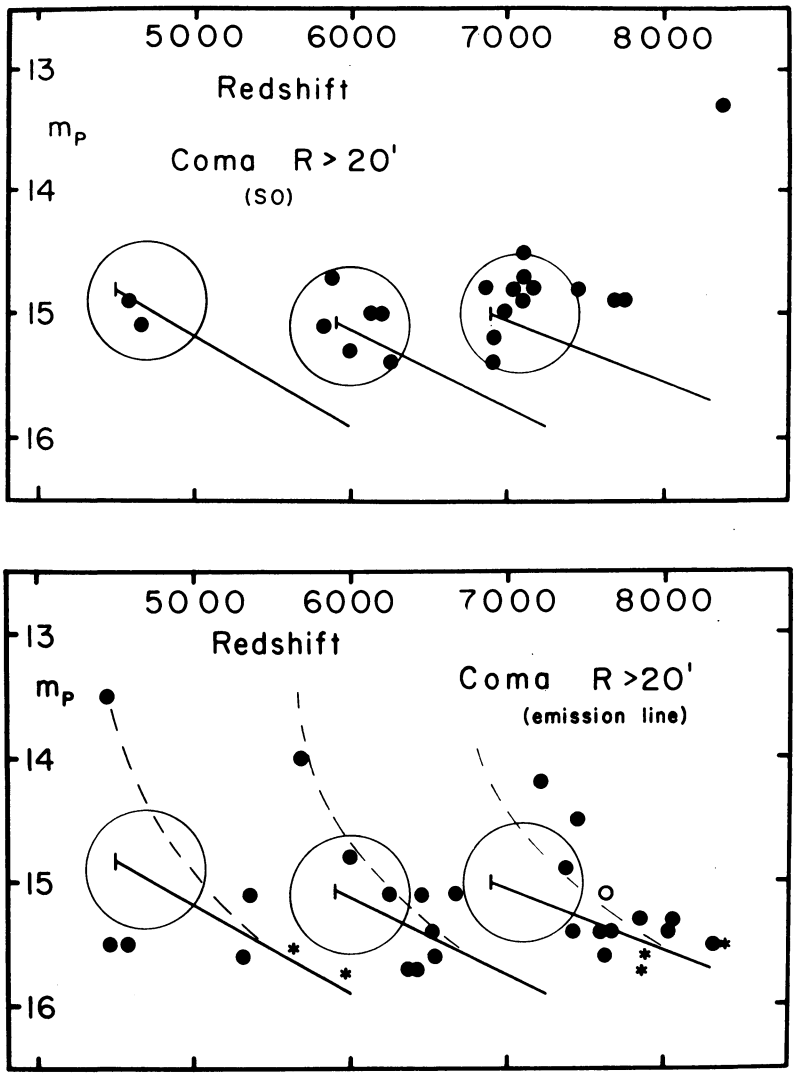

Fig. 6. (upper) Non-emission S0 galaxies in the outer part of Coma contained in the sample of objects shown in the lower part of Figure 5. The band location lines from Figure 5 are also shown. The S0 galaxies concentrate into three band-associated regions indicated by the reference circles. (lower) Emission line galaxies in the extended Coma sample (filled circles = outer Coma region, open circle = inner Coma region, * = additional new outer region data derived by S. A. Gregory at Steward Observatory, July 1973). Emission galaxies associate with the bands as do the S0 types, but are systematically shifted from the S0 regions along each band. When observed with morphological subsets, the band pattern becomes visible and a distinct band-related morphological separation in the same sense as the inner Coma investigations appears.

https://doi.org/10.1017/S0074180900024499 Published online by Cambridge University Press

1974). The upper part of the figure illustrates the location of the bands as mapped by using objects in common with the cluster core studies. Because of the relatively low accuracy of m_p magnitudes, secondary effects in galaxy luminosity, and inhomogeneities in the sample, no band effects are visible by simple inspection of the total sample. If, however, we recall that there is morphological separation along the bands, and confine our attention to specific morphological types, the bands can be made visible as shown in Figure 6. Non-emission line S0 galaxies concentrate in specific band-associated regions as do emission line galaxies. Power spectra of the redshift distributions show that the morphologic alsamples possess the known band-spacing periodicity. Band-related-morphological separation is in the same sense as seen before, later types toward higher redshift along each band. Note that one can have strong band-related-morphological separation but little or no separation in the *total* sample. Redshift-morphology studies which do not allow for multiple bands are likely to be negative or inconclusive.

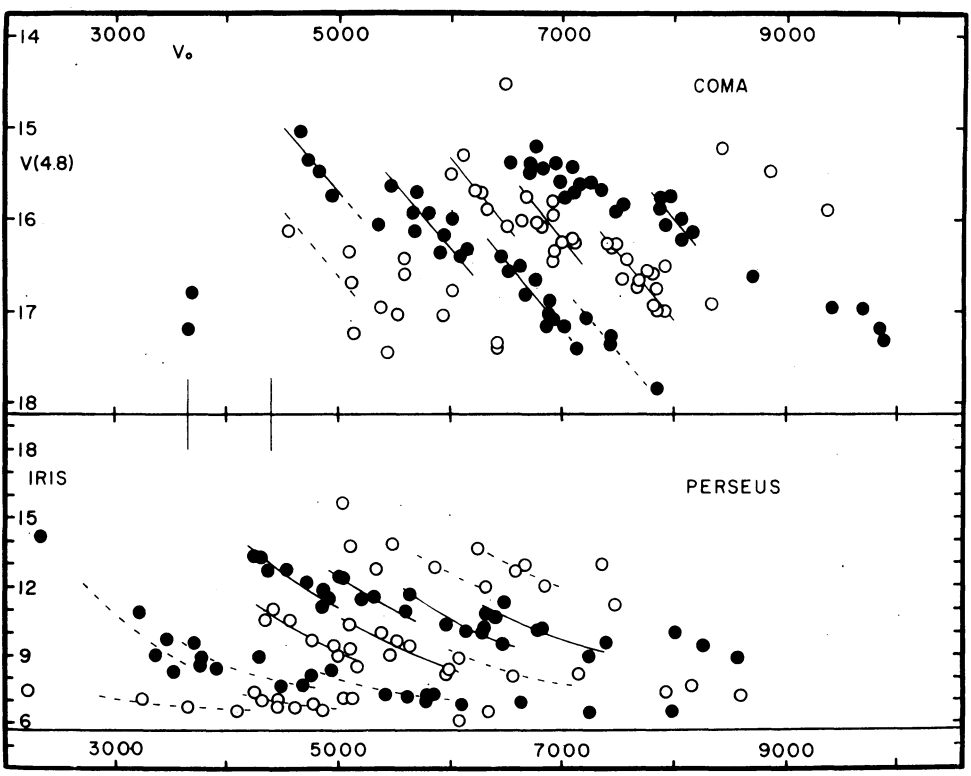

Fig. 7. 'Spin grouping' in the Coma and Perseus redshift-magnitude diagrams. The Perseus data are shown with nuclear region iris readings since magnitudes are not yet available. There is a general convergence toward the background level at 5.7. Alternate bands are indicated with different symbols. The sawtooth spin groups are shown with sloping lines, solid lines for those which appear clearly and dashed lines for other possible cases. Two vertical lines near 4000 km s^{-1} indicate the possible correspondence of band terminations in both clusters and the concentration of points on a lower band seen in Perseus but barely reached in Coma.

https://doi.org/10.1017/S0074180900024499 Published online by Cambridge University Press

The first evidence that there might be substructure within individual bands came from the extended Coma studies where a sloping sawtooth 'spin group' structuring was suggested. Figure 7 illustrates this structure for Coma and in new Perseus cluster data. Magnitudes are not yet available in Perseus, and nuclear iris photometry has been substituted. Such readings correlate closely with nuclear magnitudes (Tifft, 1973c). Since the iris index converges to the plate limit, the Perseus banding is curved and cannot yet be examined statistically as in Coma or A2199. There appears very little doubt of its reality, however, and the band spacing in redshift is greater than Coma as expected from the lower mean redshift.

It has always appeared somewhat inconsistent to me that there were discrete bands but that the distribution along the bands was continuous, except, perhaps, for the sawtooth spin grouping. A fully quantized picture with discrete states on discrete bands seemed more logical. To determine if such discrete redshift states might exist at or near the resolution limit of the data, power spectra of the redshift distributions of individual bands were considered. Unfortunately, individual bands generally contain too few points for a definitive study and some model for combining bands

$$(V_0 - C)\frac{N}{4} + C$$

$C = 6032$

$N = 2-6$

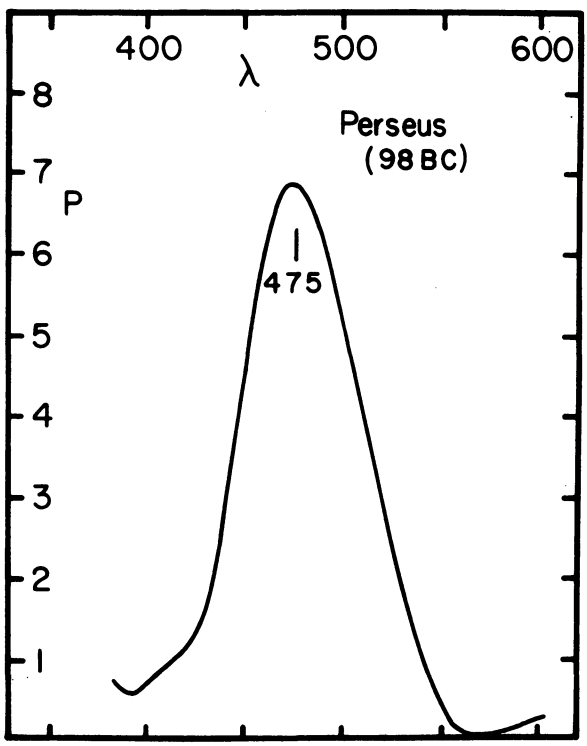

Fig. 8. Power spectrum of 98 Perseus redshifts from Chincarini and Rood (1971) = *B* or Tifft (1973c) = *C*. Redshifts have been combined after transformation by the expression given. *C* in the expression (which is unrelated to the redshift reference *C* above) is a common zero point and *N* is a sequential band number. Thus all bands are scaled to refer to band 4. When this combination procedure is followed, a modest power spectrum peak is found for a redshift interval $\lambda \equiv 474$ km s^{-1}.

was required. The first model developed was based upon the fact that superficially the spin group length appeared to vary with band number in such a way that by numbering the bands sequentially toward higher redshift from an appropriate origin, the spin group length times the band number was roughly constant. Figure 8 illustrates what happens when the Perseus bands are combined with such scaling about a common zero point. A modest power peak is produced with some phased contribution from each band.

By itself the Perseus band-related-periodicity has no significance, considering that the power is not exceptionally large and there is choice of the parameter C and origin of n. The interesting test of this concept came by applying the identical relationship to Coma and A2199 as independent samples. Figure 9 shows that both Coma and A2199 have substantial power peaks near the predicted frequency. There is a slight

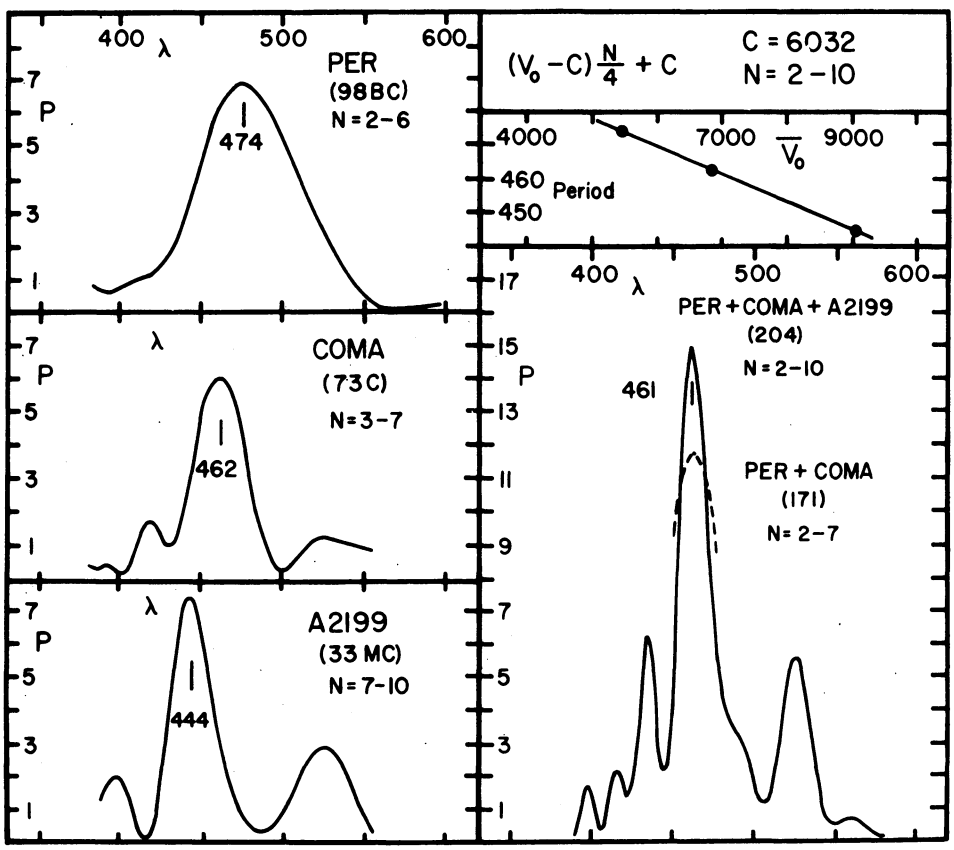

Fig. 9. Power spectra of Perseus, Coma, and A2199 redshift distributions are shown on the left. Galaxies have been combined according to band number using the expression at top right as discussed in Figure 8 and the text. The individual cluster power spectra show peaks which shift slightly with mean cluster redshift as shown on the right. The combined cluster power spectrum is shown at lower right. In calculating these power spectra, older redshifts tabulated by de Vaucouleurs and de Vaucouleurs (1964) and values from Kintner (1971) have been omitted, since they contain some large scatter.

https://doi.org/10.1017/S0074180900024499 Published online by Cambridge University Press

smooth systematic drift with mean cluster redshift. Finally, when the three cluster samples were combined in a single analysis to test the relative phasing of the periodicity in the individual clusters, the result was a powerfully reinforced peak of power level 15. This reinforcement has, of course, to be present if the concept of a universal intrinsic redshift is valid.

My interpretation of the observed periodicity is not that the model is correct in detail, but that it represents an interference effect of a real band-related-periodicity still not directly visible. To observe a true discrete periodicity, which I was now convinced existed, a precision redshift sample was required. Such a sample was generated

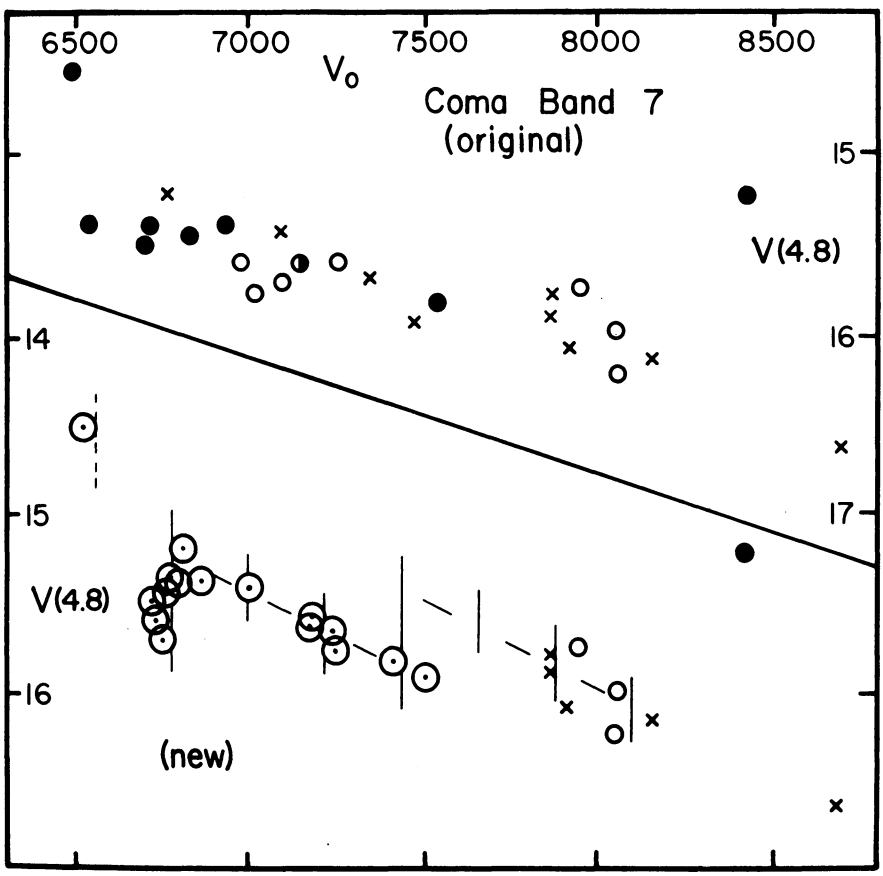

Fig. 10. Galaxies on and above the brightest Coma cluster band. The upper figure shows the band with the original, previously published redshifts (filled circles = de Vaucouleurs and de Vaucouleurs (1964), open circles = Kintner (1971), X = Tifft (1972, 1973a), composite symbols = means of two sources). In the lower figure the redshifts below 7600 km s^{-1} have been replaced by accurate new mean redshifts from multiple spectrograms. The symbol size indicates the one sigma redshift uncertainty of about 35 km s^{-1}. Reduction is incomplete above 7600 km s^{-1} so the upper symbols are repeated. Some of the older redshifts contained errors in excess of 300 km s^{-1}. The new values show both the 'spin grouping' sawtooth wave on the band (dashed lines) and a 220 km s^{-1} 'spin state' periodicity (vertical lines).

by observing each member of the brightest Coma band three times independently. Most of these galaxies had redshifts from other sources, some of doubtful accuracy. This band also was the only one in Coma not showing clear spin grouping.

Figure 10 shows the original and new accurate Coma band 7 redshift-magnitude diagrams. The data are at present complete only for the 16 bright objects where the

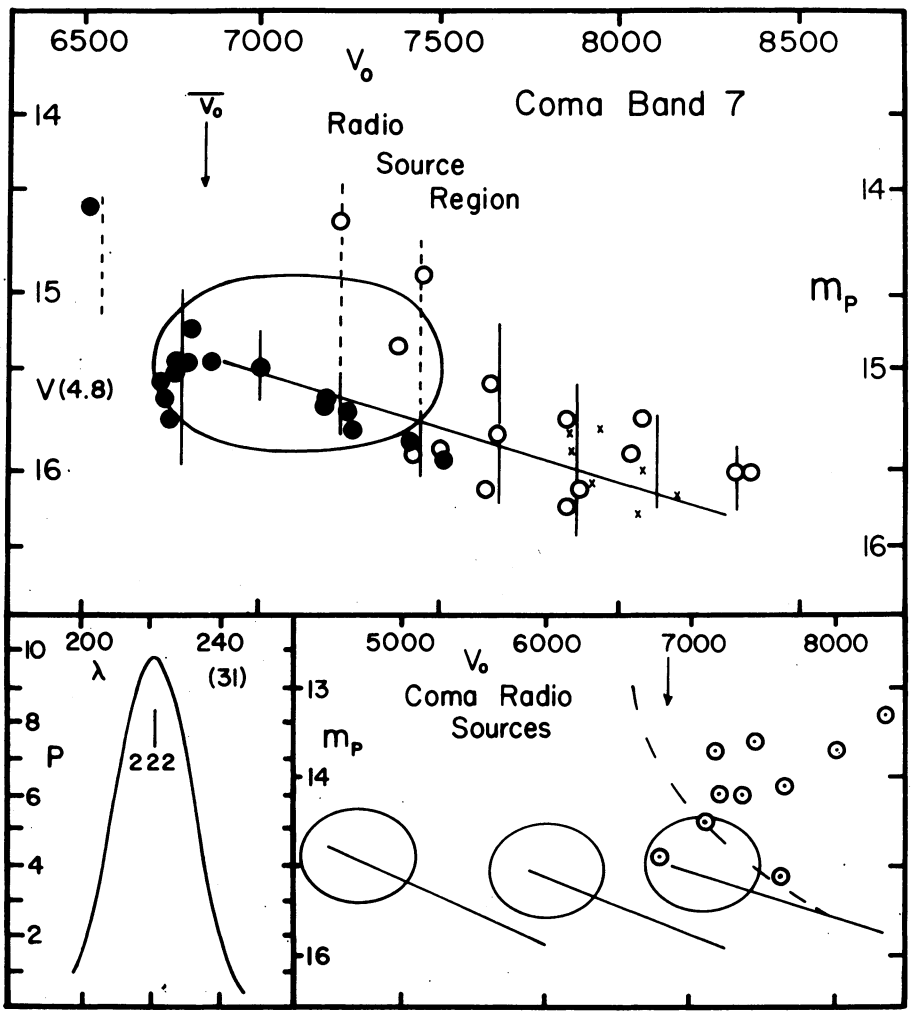

Fig. 11. (upper) Composite Coma band 7 with filled circles for the accurate data from Figure 10 and open circles for emission-line objects from the upper band in the lower part of Figure 6. Some of the lower accuracy data from Figure 10 are shown with small X symbols. The left-hand scale is $V(4.8)$ from Figure 10 and the right-hand scale is m_p from Figure 6 shifted for a rough match. The m_p band line and S0 reference region are repeated for comparison. The 'spin state' periodicity is shown with vertical lines. (lower) The power spectrum of the redshift distribution of the filled and open circle data is shown at the lower left. At the lower right the location of the 5C Coma radio sources is shown (Willson, 1970). They fall directly above the band and well above the mean cluster redshift, shown with a vertical vector.

https://doi.org/10.1017/S0074180900024499 Published online by Cambridge University Press

radii of the circles represent the 35 km s^{-1} mean internal error in the final redshifts. Errors in some of the original redshifts exceeded 300 km s^{-1}. Both the spin grouping sawtooth and a rather clear 220 km s^{-1} discrete 'spin state' periodicity are now visible.

Since 16 objects were not really enough for a good power spectrum test, I added to the sample the Coma emission-line galaxies, previously discussed, which were assigned to the same band. Emission-line redshifts are generally fairly accurate. Figure 11 shows the composite accurate Coma band 7 picture and its power spectral analysis, which gives a peak power of 10 at the 222 km s^{-1} spin state periodicity. The probability of accidentally finding such a peak is 10^{-3}.

Figure 11 contains some intriguing information on band-related morphology and periodicity. Note that the bright group of ellipticals represent one spin grouping and this corresponds perfectly with the location of the outer Coma S0 concentration. The next spin group consists of non-ellipticals in the inner region and is the main concentration region for outer Coma emission line galaxies. Thus morphology appears closely tied to spin grouping. Pervading all is the 220 km s^{-1} spin state periodicity. We now have a concept of discrete 'spin states' organized into 'spin groups' and 'bands', and perhaps bands into band systems – a totally non-Doppler intrinsic redshift picture which I suggest has its origin in multiple substates of matter itself. One number of interest, the redshift dispersion about the set of discrete states is about 40 km s^{-1}, scarcely larger than the internal redshift uncertainty of about 35 km s^{-1}. An upper limit of about 20 km s^{-1} on real Doppler motion of galaxy nuclei within clusters is implied.

In order to produce the apparent observed pattern of redshift increase with distance, we can invoke systematic cosmic time dependent evolution of matter which we then see displayed in lookback time. The focus of this evolution is, I believe, galaxy nuclei. There are, apparently, conditions in nuclei of galaxies which process, create, or somehow operate on matter systematically with cosmic time. Matter may undergo transitions between states being systematically collapsed, possibly by great gravitational compaction, into progressively more tightly bound configurations with the systematic release of positive energy. Galaxies – the visible outflow products of these nuclei – can be systematically removed from the high redshift (low energy) end of a distribution with energy released in the process. The inset in Figure 11 shows how the Coma radio sources all lie above the high redshift band, and I suggest that the energy source of such radio objects arises from matter state transitions.

Because of the remarkable uniformity in redshift-magnitude diagram details, I suspect that nuclei must also be considered as certain 'standard' units in themselves, not simply random lumps of matter. Any explanation of multiple states of matter presumably resides in the realm of nuclear physics and the structure of fundamental particles.

References

Chincarini, G. and Rood, H. J.: 1971, *Astrophys. J.* **168**, 321.

de Vaucouleurs, G. and de Vaucouleurs, A.: 1964, *Reference Catalogue of Bright Galaxies*, University of Texas Press, Austin.

Kintner, E. C.: 1971, *Astron. J.* **76**, 409.
Tifft, W. G.: 1972, *Astrophys. J.* **175**, 613.
Tifft, W. G.: 1973a, *Astrophys. J.* **179**, 29.
Tifft, W. G.: 1973b, *Astrophys. J.* **181**, 305.
Tifft, W. G.: 1973c, *Astron. J.* **78**, 594.
Tifft, W. G.: 1974, *Astrophys. J.* **188**, 221.
Willson, M. A. G.: 1970, *Monthly Notices Roy. Astron. Soc.* **151**, 1.

Acknowledgement

Figures in this paper are reproduced from *The Astrophysical Journal*; Copyright: The American Astronomical Society, by permission of the University of Chicago Press.

DISCUSSION

B. Peterson: Would you describe the method and equipment used to obtain the nuclear magnitudes for the Coma cluster?

Tifft: The Coma nuclear magnitudes are from the Rood and Baum studies (*Astron. J.* **72**, 398 1967; **73**, 442, 1968). These were based upon tracings taken from 200-in. calibrated V photographs and were tied to photoelectric observations for the zero point. Unpublished portions of the Rood-Baum photometry should be available soon, probably in *Astrophysical Journal Supplements*. The m_p magnitudes in my outer Coma studies are from the catalogue of Zwicky and collaborators. All my own redshifts are from 90-in. Steward Observatory image tube spectra at 240 Å mm^{-1} and have an internal rms uncertainty of about 60 km s^{-1} on bright galaxies, and about 100 km s^{-1} on faint objects. There are good comparisons of my redshifts with new Gunn and Sargent data in Coma. The agreement is excellent.

Freeman: If the redshifts you used came from the whole Galaxy rather than just the nucleus, would this affect your argument significantly?

Tifft: If we take seriously the concept that nuclei could undergo 'transitions' in redshift, there might well be a systematic difference between 'nuclear' and 'envelope' redshifts in some cases. In fact the envelope of E type galaxies is virtually impossible to observe for redshift, and all present values are 'nuclear'. It is also quite possible that multiple redshifts (nuclear-envelope) might only be briefly observable. Envelopes might dissipate – to be really far out but not impossible, one might postulate gravitational decoupling of states which would lead to rapid dissipation of envelopes and a complete replacement of the galaxy in a 'new' state. Seriously, the important problem is to proceed with good solid data and tests, and minimize the interpretations.

Freeman: Three bands in Coma converge at approximately zero redshift and $V = 12$. Has this any particular significance?

Tifft: Not to my knowledge. The QSS bands seem to converge to a similar value.

Lewis: Comparison of the 21-cm velocities with the optical systemic velocities gives a reasonable test for differences between the disk and the nucleus. The 21-cm velocity is an average velocity from gas over the whole disk, while the optical velocity generally represents the velocity of the nucleus only. Roberts showed (*IAU Symp.* **44**, 12, 1972) that the regression V_{21} against V_{optical} for about 130 galaxies had no systematic residual.

Following Tifft's (*Astrophys. J.* **175**, 613, 1972) result on the core of the Coma cluster, I examined the magnitude and velocity data for the *whole* Coma cluster, to look for evidence of non-Doppler redshifts. There are 197 galaxies with velocities satisfying $3000 < V < 10000$ km s^{-1} and with types quoted in Rood *et al.* (*Astrophys. J.* **175**, 627, 1972), Tifft (*Astrophys. J.* **179**, 29, 1973), and Tifft and Gregory (*Astrophys. J.* **181**, 15, 1973). Self-consistent magnitudes m_p are adopted from these papers or derived from Figure 5 of Tifft (1972) after an upward adjustment of 0.7 mag. Table I lists the mean data for all 197 galaxies in rows (1) and (5), as well as the means for Mayall's (*Ann. Astrophys.* **23**, 344, 1960) statistically uniform selection of bright galaxies in rows (2) and (6) and the non-Mayall sample means in rows (3) and (7). These figures suggest that

(i) the largest velocity difference between E and non-E or S0 galaxies is (221 ± 222) km s^{-1} (row 1).

(ii) a 200 km s^{-1} uncertainty exists in the mean velocity of any type. This appears in the differences listed in row (4) between the Mayall and non-Mayall samples.

(iii) Mayall's sample is 1.3 to 1.5 mag brighter than the non-Mayall sample (row 8).

(iv) with these magnitude differences, Tifft's redshift-magnitude relations predicts the velocity differences in row (9). These disagree with the observed values in row (4) by a factor of ten.

(v) $\bar{m}_{S0} - \bar{m}_E = (0.48 \pm 0.22)$ mag from row (5). If the brighter ends of all Tifft's bands are preferentially populated by elliptical galaxies, Tifft's redshift-magnitude relation should be applicable. It

TABLE I

Average systemic velocity and magnitude of Coma cluster galaxies

Sample	Datum	E	S0	Non-E	Units
(1) Total sample	(a)	6728 ± 98	6949 ± 124	6880 ± 110	km s^{-1}
	N	78	95	118	
(2) Mayall's sample	(a)	6828 ± 138	6786 ± 191	6662 ± 155	km s^{-1}
	N	33	23	39	
(3) Non-Mayall sample	(a)	6652 ± 135	7001 ± 149	6952 ± 142	km s^{-1}
	N	45	72	79	
(4) row (3) – row (2)	$\overline{\Delta V}$	-176 ± 273	$+215 \pm 340$	$+290 \pm 297$	km s^{-1}
(5) Total sample	(b)	15.25 ± 0.12	15.73 ± 0.10	15.55 ± 0.10	m_{pg}
	N	78	95	118	
(6) Mayall's sample	(b)	14.49 ± 0.10	14.63 ± 0.12	14.55 ± 0.09	m_{pg}
	N	33	23	39	
(7) Non-Mayall sample	(b)	15.81 ± 0.11	16.09 ± 0.09	16.05 ± 0.09	m_{pg}
	N	45	72	79	
(8) row (7) – row (6)	$\overline{\Delta m}$	1.32 ± 0.21	1.46 ± 0.21	1.50 ± 0.18	m_{pg}
(9) (row (3) – row (2)) calc.	ΔV	2200 ± 350	2400 ± 350	2500 ± 300	km s^{-1}

(a) $\langle V \rangle \pm \sigma(V)/\sqrt{N}$; (b) $\langle m \rangle \pm \sigma(m)/\sqrt{N}$.

predicts a velocity difference of $(+800 \pm 370)$ km s^{-1}.

These data do not confirm Tifft's fundamental hypotheses. The data for the whole Coma cluster suggest that $\bar{V}_{S0} - \bar{V}_E \lesssim +200$ km s^{-1}.

Tifft: The critical question is the association of morphology with redshift within *individual* bands compared with the total sample. Since several bands are present and they overlap in redshift, it is not clear that morphological separation should appear in mean overall redshift even if it were very strong in individual bands. This is quite obvious in my figure comparing S0 and emission line galaxies. A distinct shift in morphology occurs *on each band* but is insignificant in the overall average. It may be accidental that the total core sample shows the effect so well. Individual bands show it much more clearly and at *all* radii.

A second important factor concerns changes in the sample for different radial regions about the cluster. There are definite changes in average morphology with radius. Outlying galaxies may be poor objects to examine in a search for an *identical* correlation as seen in the core region. For example, the outlying E galaxies include 'blue' and active (emission, radio) objects to a higher degree than inner region E types. It is dangerous to consider them to be comparable for mean redshift or magnitude tests. The outer sample is also incomplete, while the core region is complete to some specified magnitude.